Chemical Composition of Carbonatite Minerals in Karasug Deposit, Tuva

A. V. Bolonin[1] and A. V. Nikiforov

Institute of Geology of Ore Deposits, Petrography, Mineralogy, and Geochemistry (IGEM),
Russian Academy of Sciences, Staromonetnyi per. 35, Moscow, 119017 Russia
Received April 20, 2004

Abstract—Results of electron microprobe analyses (70 determinations) of minerals in the Karasug deposit of complex ores (Fe, F, Ba, Sr, TR, U, and Mo) in Tuva are presented. The chemical compositions and other properties of minerals are characterized taking into account earlier published data for barren ankerite–calcite carbonatites (calcite, ankerite, dolomite, apatite, monazite, parisite, thorite, pyrite, rutile, and strontianite) and ore-bearing fluorite–barite–siderite carbonatites (siderite, fluorite, Ba and Sr sulfates, bastnaesite, hematite, pyrite, molybdenite, uraninite, and muscovite). The inhomogeneity of mineral compositions in dolomite–ankerite, parisite–synchisite, and barite–celestine associations is imaged in reflected electrons. A summary of published data on Ba and Sr sulfates shows that the natural compositions of these isomorphic minerals correspond to the following separate groups: barite–Sr-barite–barytcelestine–Ba-celestine–celestine. Some conclusions are drawn regarding the typomorphic features of the mineral compositions for the carbonatites.

INTRODUCTION

The Karasug deposit of complex ores is located in the Altai–Sayany folded region on the territory of Central Tuva. The local population in Tuva used limonite ochre from this deposit from ancient times. The deposit was mentioned for the first time in 1917, when the paper "Copper Ores of Uryankhai" by mining engineer B.M. Porvatov was published in *Vestnik Obshchestva Sibirskikh Inzhenerov* (Bulletin of the Society of Siberian Engineers). The deposit was explored in two stages: in 1947–1954 by the Mining Expedition, headed by A.S. Mitropolskii, and in 1979–1984 by the Berezovsk Prospecting–Geological Enterprise (G.M. Komarnitskii, V.K. Maksimov, and others). The problems of geological structure, mineralization, and deposit origin were considered in papers by Mitropolskii (1959, 1962), Khomyakov (1964), Ontoev (1984), and others. Bolonin (1987, 1999) noted that carbonate associations in the deposit, represented by ankerite–calcite and fluorite–barite–siderite rocks, are of injection–magmatic genesis. The fluorite–barite–siderite carbonatites enclose complex ores that consist 95% of commercial minerals. However, published information on their chemical compositions is rare and is based on chemical analysis of their monofractions only.

This paper presents data for the mineral compositions in two carbonatite samples, analyzed with an ABT-55 scanning electron microscope (Japan) and a LINK AN-10000/85S x-ray spectrometer (Institute of Geology and Geochronology of the Precambrian RAN; analysts: M.D. Tolkachev and M.R. Pavlov; accelerating voltage 25 kV, beam current 1 nA), as well as sum-marizes information on chemical compositions and other mineral properties obtained from other sources.

BRIEF GEOLOGICAL CHARACTERISTICS OF THE DEPOSIT

A series of Late Mesozoic carbonatites (preliminary Rb–Sr isochronous data of the authors) is distinguished on the territory of Central Tuva in terrigenous Lower and Middle Paleozoic sediments. The northern group of carbonatite bodies, with an area of about 20 km², is known as the Karasug ore field or deposit. Carbonatite bodies of pipelike and dikelike form are confined to thick fault zones or to their intersections (Fig. 1). The sizes of the carbonatite bodies are various. The two largest bodies have a diameter of more than 500 m. The thickness of linear bodies is up to 100–160 m, and their length is several hundred meters. Carbonatites have subvertical intersecting contacts with host rocks.

The carbonatite bodies are composed of ankerite–calcite carbonatites of the first intrusion phase and of fluorite–barite–siderite carbonatites of the second intrusion phase. Brief information on mineral compositions of rocks and their textures and structures is presented in Table 1. The fluorite–barite–siderite carbonatites either form independent bodies or cut the earlier ankerite–calcite carbonatites as semicircular dikes. Some carbonatite bodies include remnants of brecciated and greisenized granitoids (Fig. 1). In addition, carbonatites are saturated with relatively small angular fragments of host sandstones, siltstones, and granitoids. Fragments of earlier crystallized ankerite–calcite carbonatites are also observed in rocks of the second intrusion phase. The form of carbonatite bodies, their tex-

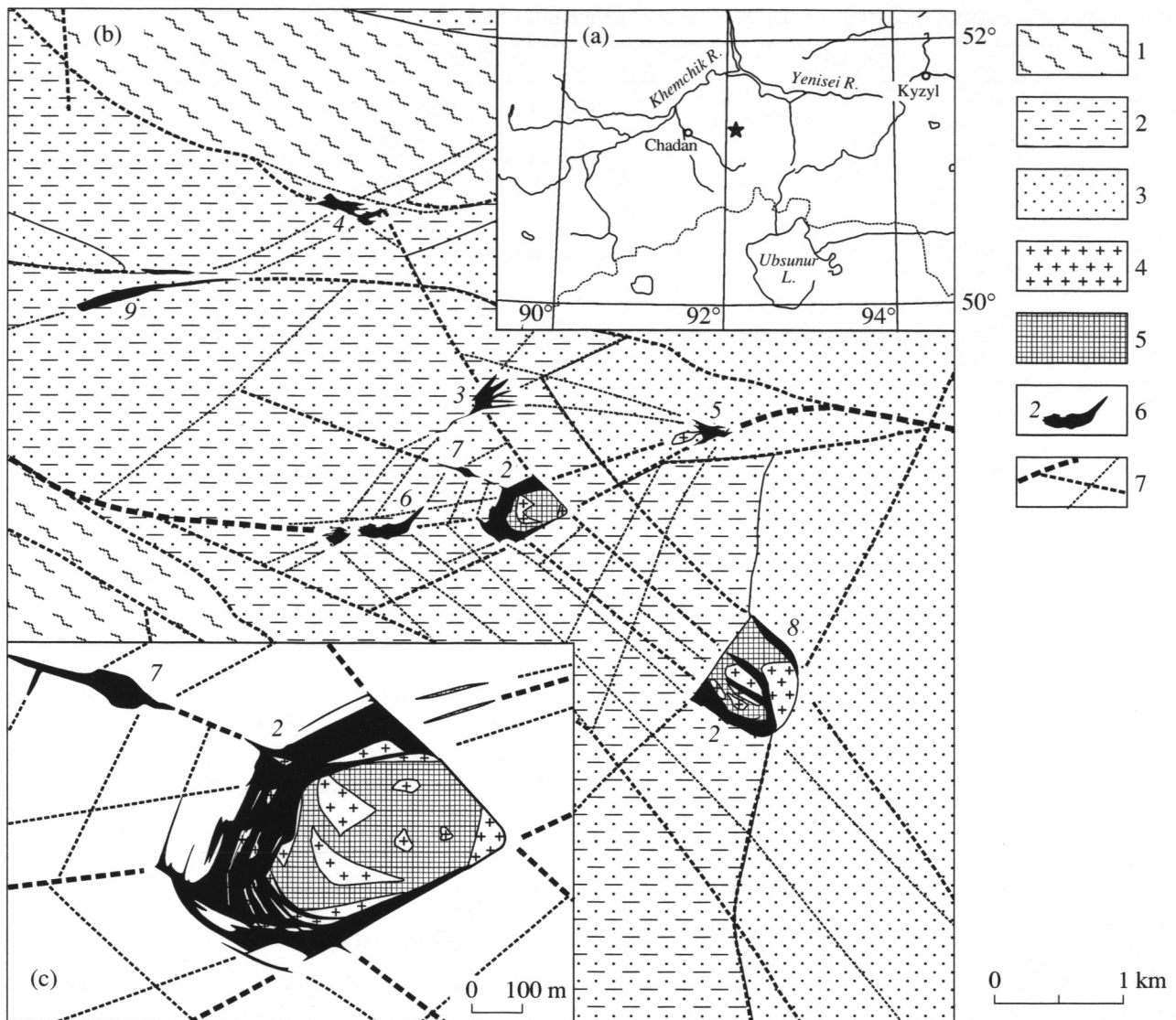[1]Corresponding author: A.V. Bolonin. E-mail: nikav@igem.ru

Fig. 1. Geographic location (a) and geological–structural scheme of the Karasug ore field (b) and areal view of the second orebody (c). Prepared on the basis of data of A.S. Mitropolskii and V.K. Maksimov. (1) Lower Cambrian basement: schists, sandstones, limestones, and porphyrites; (2) Ordovician sandstones, siltstones, and conglomerates; (3) Silurian sandstones, siltstones, and marls; (4) granites; (5) ankerite–calcite carbonatites; (6) orebodies of fluorite–barite–siderite carbonatites and their numbers; (7) faults of various scales.

tures and structures, and the character of contacts with host rocks indicate their magmatogene origin.

The postmagmatic hydrothermal–metasomatic mineralization is widely manifested within fluorite–barite–siderite carbonatites, in contrast to ankerite–calcite carbonatites (Table 1). It is expressed in a wide development of hematite along linear zones in association with late bastnaesite. Hematite is one of the main rock-forming minerals in carbonatites. Furthermore, replacement of barite by late barium and strontium sulfates and the development of quartz–siderite and celestine veinlets are observed at a number of sites in fluorite–barite–siderite carbonatites. The local silicification of rocks is characteristic for both carbonatite varieties.

In the Pre-Oligocene, the carbonatites (Mitropolskii, 1962) experienced intense hypergene oxidation to a depth of 100–300 m with the formation of an "iron cap." As a result, some minerals in carbonatites were subjected to complete annihilation (siderite, ankerite, sulfides, magnetite, and uraninite) and were replaced mainly by Fe hydroxides and some other minerals were transformed (barytcelestine), while remaining minerals were practically intact (calcite, hematite, fluorite, barite, bastnaesite, parisite, monazite, apatite, quartz, muscovite, and rutile). Due to ankerite oxidation, the ankerite–calcite carbonatites acquired a characteristic spotted color, and the fluorite–barite–siderite carbonatites and their derivatives were transformed into highly

Table 1. Mineral associations, textures, and structures of cabonatites of the Karasug deposit

Mineral-forming processes	Magmatic		Postmagmatic autometasomatism			
	First intrusion phase	Second intrusion phase	hematitization	celestinization	silicification	veinlets
Main textures	Breccia-like, massive	Breccia-like, massive, banded	Impregnated–pocketed, banded	Impregnated–pocketed	Impregnated–pocketed	Veinlet
Main structures	Hypidiomorphic, porphyraceous	Porphyraceous: impregnations and ground mass	Metacrystalline	Corrosional	Corrosional	
Ankerite–calcite carbonatites	Calcite 45–60% Ankerite 35–50% Apatite 1–2% Quartz I 1–2% Pyrite 0.5–1.5% Monazite up to 0.5% Parisite up to 0.5% Roentgenite Muscovite Rutile Magnetite Thorite Molybdenite Chalcopyrite	Celestine	Hematite up to 30% Bastnaesite Magnetite		Quartz up to 20%	
Fluorite–barite–siderite carbonatites		Siderite I + II 61% Barite 20% Fluorite I + II 12% Pyrite I + II 3% Bastnaesite I 1–1.5% Quartz I 1% Apatite Molybdenite I up to 0.03% Uraninite I up to 0.03% Magnetite I Muscovite Rutile	Hematite up to 60% Bastnaesite II 0.5–1% Pyrite III up to 5% Magnetite II up to 0.5%	Barytcelestine up to 25% Ba celestine up to 5% Celestine I Sr barite Fluorite III up to 5% Quartz I Pyrite IV Chalcopyrite I Molybdenite II Sphalerite I Galenite I Uraninite II	Quartz III up to 50%	Celestine II Quartz IV Siderite III Fluorite IV Bastnaesite III Pyrite V Marcasite Chalcopyrite II Molybdenite III Sphalerite II Galenite II Uraninite III

porous dark brown hematite–goethite or yellow–brown limonite varieties. The strontianite mineralization was widely developed in the oxidation zone among unoxidized carbonatites. White and yellowish white radial–asterial acicular strontianite crystals form pocketlike metasomatic intergrowths and fill small veinlets of various orientation. Light blue celestine is observed in veinlet selvages, nodular hydrogoethite is found at the edges of crystal growth, and transparent calcite occurs in the center. The hypergene minerals are not considered in this paper.

The fluorite–barite–siderite carbonatites and their derivates were explored as complex ores. The extrac-

tion technology for fluorite and fluorine (HF), barite and barium ($BaCl_2$), iron concentrate, rare earths, strontium, uranium, and molybdenum was developed at the All-Russia Institute of Mineral Resources using laboratory samples for oxidized and unoxidized (primary) ores of the deposit (V.E. Lifirenko, N.V. Petrova, E.P. Nikolaeva, and others, 1983).

MINERAL COMPOSITION OF CARBONATITES

Fluorite–Barite–Siderite Carbonatites

The primary mineral composition, textures, and structures of fluorite–barite–siderite carbonatites are
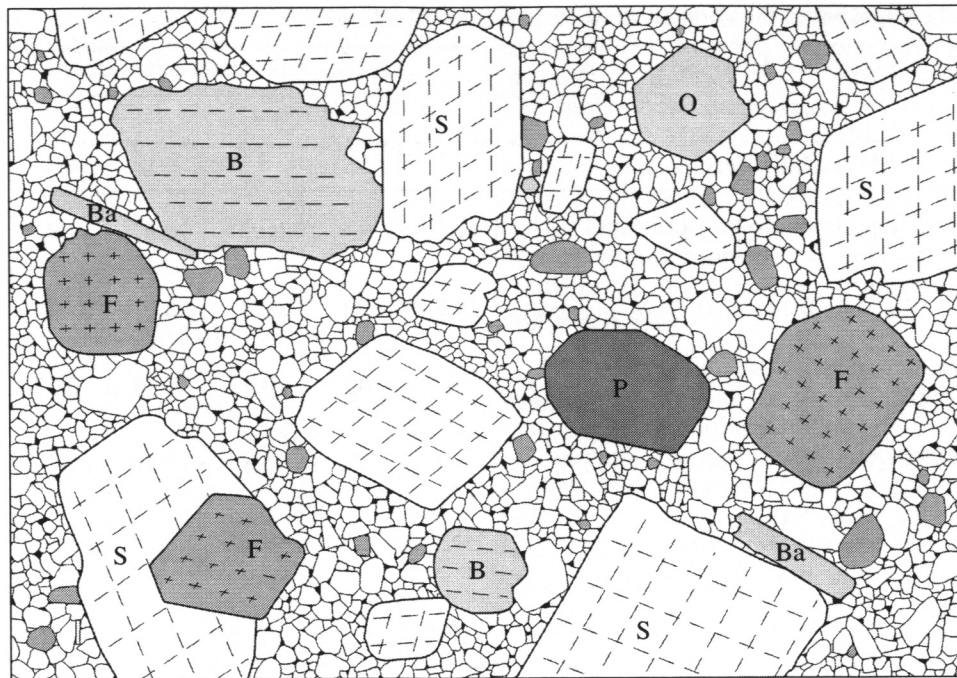
Fig. 2. The primary porphyraceous texture of fluorite–barite–siderite carbonatites. Magnification 10. Minerals in impregnations: S, siderite; F, fluorite; B, barite; P, pyrite; Q, quartz; Ba, bastnaesite. Ground mass, an allotriomorphic fluorite–siderite aggregate.
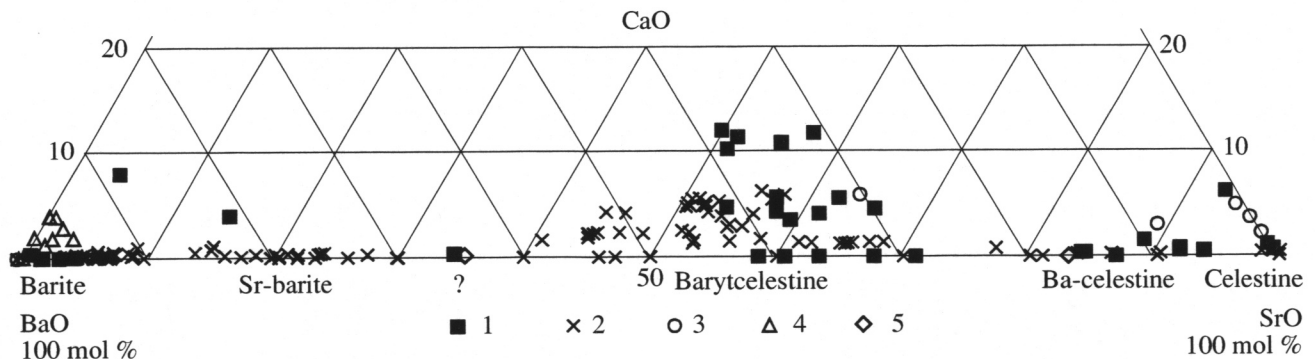

Fig. 3. Content of Ba, Sr, and Ca in sulfates of the barite–celestine series. (1) Karasug deposit (37 analyses); (2) Late Mesozoic carbonatites of the Western Transbaikal region (104 analyses); (3) Mushugai complex, Mongolia (5 analyses); (4) deposits in Georgia (10 analyses); (5) deposits in Turkey (2 analyses).

relatively consistent in large bodies. The average mineral composition of these rocks is as follows (wt %): siderite, 61; barite, 20; fluorite, 12; pyrite, 3; bastnaesite, 1–1.5; quartz, 1; apatite, 0.5; molybdenite, 0.03; and uraninite, 0.02. Magnetite, muscovite, and rutile are also observed, the total content of which does not exceed 1 wt %. The rocks are characterized by porphyraceous texture, when large impregnations of siderite, fluorite, barite, pyrite, and quartz are disseminated in a fine-grained (<0.2 mm) ground mass (Fig. 2). Intracrystallization and late cataclasis of rocks are widely manifested.

The fluorite–barite–siderite carbonatites are rarely preserved in their primary form. Their composition is variously modified by minerals of superimposed associations and by fragments of host aluminosilicate rocks, sometimes partially reworked. The primary complex ores, which did not undergo hypergene oxidation, have the following average mineral compositions (wt %): siderite, 37–39; barite, 12–13; hematite, 10–12; fluorite, 9; barytcelestine, 5–7; pyrite, 2.5; bastnaesite, 1.7; strontianite, 1; apatite, 0.5; and quartz and aluminosilicate rocks in fragments, 16–18. Magnetite, celestine, muscovite, rutile, molybdenite, and uraninite are insignificant, and chalcopyrite, sphalerite, galenite, and marcasite are sporadic. The occurrence of feldspars, quartz, mica, chlorite, clay minerals, calcite, ankerite, zircon, monazite, parisite, orthite, and thorite is associated with

Table 2. Chemical compositions of carbonatites, wt %

Oxides	Fluorite–barite–siderite carbonatites					Ankerite–calcite carbonatites					
	siderite					ankerite I			ankerite II		
		4-9	4-10	4-6		8-3	8-5	8-12	8-1	8-2	7-3
MgO	1.0(6) / 0.7–1.5	1.1	0.66	1.1	0.96(7)* / 0.56–1.26	11.0	9.8	10.9	10.9	1.9	4.0	1.5
CaO	0.7(6) / 0.3–1.0	0.97	0.34	0.78	0.72(7) / 0.4–1.71	28.9	29.1	29.8	28.9	28.0	27.1	27.4
MnO	0.9(6) / 0.5–1.4	0.58	1.4	0.71	1.35(7) / 0.97–1.62	0.41	0.33	0.41	0.39	0.27	0.42	0.33
FeO	59.5(6) / 57.9–61.1	59.5	61.1	60.5	58.7(6) / 57.8–59.5	13.6	16.0	14.8	15.9	28.5	26.4	28.1
SrO	0.15(6) / 0.1–0.2	0.09	0.18	0.18		0.30	0.31	0.27	0.27	0.12	0.12	0.12
BaO					0.02–0.35							
SiO_2	0.1	0.15	0.12	0.07	0.1	0.20	0.16	0.15	0.17	0.16	0.14	0.08
Al_2O_3	0.1	0.17	0.12	0.01	0.47–0.89	–	–	–	–	–	0.02	0.02
TR_2O_3	<0.1	0.05	0.08	0.16	0.12	0.21	0.01	0.10	0.04	0.09	0.03	–

Oxides	Ankerite–calcite carbonatites												
	ankerite II				dolomite					calcite		Mg-siderite	
	8-6	8-4	8-11	8-13		8-10	8-9	8-8	8-7		7-1	7-2	
MgO	2.6	1.7	1.4	2.1	16.1	17.3	17.8	19.3	16.8	0.1(4)	0.04	4.4	3.9
CaO	26.8	27.7	27.6	26.4	34.3	34.3	33.7	32.2	34.0	55.1(4) / 54.3–56.1	54.9	1.4	2.1
MnO	0.47	0.35	0.27	0.38	0.08	0.12	0.03	0.10	0.16	0.2(4) / 0.1–0.4	0.09	0.73	0.64
FeO	28.6	29.2	29.1	29.2	1.7	2.1	2.1	2.4	2.0	0.8(4) / 0.5–1.0	0.99	56.2	53.6
SrO	0.04	0.20	0.13	0.07	0.59	0.39	0.38	0.49	0.50	0.1(4) / <0.1–0.3	0.31	0.14	0.106
BaO													
SiO_2	0.12	0.21	0.19	0.11	0.14	0.07	0.16	0.32	0.09	0.1	0.12	0.09	0.11
Al_2O_3	0.10	0.07	0.09	0.11	–	–	–	0.03	–	0.1	0.06	–	0.01
TR_2O_3	–	0.11	0.10	0.17	0.07	0.11	0.22	0.07	0.14	0.1	0.16	0.04	0.03

Note: Numerator, average contents and numbers of analyses (in parentheses); denominator, maximum and minimum contents.
  * According to data of chemical analysis of mineral monofractions from A.S. Mitropolskii, D.O. Ontoev, and A.P. Khomyakov. Blanks, element was not determined; dashes, it was not found; 4-9, 4-10, and so on are sampling points.

fragments of host rocks and ankerite–calcite carbonatites in ores.

Siderite is the main rock-forming mineral of ore-bearing carbonatites and, at the same time, the major commercial iron mineral in ground ores. Quantitatively, it is approximately equally distributed between impregnations and the ground mass. The form of impregnations is rhombohedral; their size varies from 0.2 to 10 mm, with that of single crystals being up to 4 cm. The mineral color is white with a yellow or green shade; the parameters of the unit cell are as follows: $a = 4.692$ Å, $c = 15.384$ Å, density 3.88 g/cm^3. In the primary mass, the siderite composes light gray fine-grained (0.0n–0.2 mm) aggregates of rounded and angular grains. The chemical compositions of siderite impregnations are presented in Table 2. The data of

Table 3. Chemical compositions of fluorite from the fluorite–barite–siderite carbonatites, wt %

Components	Fluorite I		Fluorite II		
F			47.3*		
CaO	68.4	74.6	70.6	74.4	70.2
MgO	–	–		0.01	0.07
MnO	0.03	0.06		–	–
FeO	–	0.04		0.18	0.48
SrO	0.03	0.12	0.2–0.5	0.14	–
BaO			0.06–0.5		
SiO$_2$	0.19	0.11	0.16	1.6	0.23
TiO$_2$	0.02	–		0.07	–
Al$_2$O$_3$	0.10	0.06	1.1	0.03	0.06
Y$_2$O$_3$	0.10	0.21	0.09	0.11	0.15
TR$_2$O$_3$	0.20	0.21	0.5	0.10	0.48

* Data of A.S. Mitropolskii and A.P. Khomyakov.

scanning electron microscope and microprobe determinations indicate that the cation composition of mineral in impregnations and in the primary mass is identical. The mineral is characterized by insignificant admixtures (wt %): MnO, 0.9–1.3; MgO, 1.0; and CaO, 0.7. In the oxidation zone, siderite is completely replaced by Fe hydroxides (hydrogoethite and goethite), which form pseudomorphs of porous–cellular structure. Due to such pseudomorphs, the porosity of oxidized ores increases to 20–25 vol % in comparison with 5–8 vol % in primary ores.

Fluorite content varies in the range 1–20% according to data of run-of-the-mine ore sampling performed during deposit exploration; its content is 6–12% in half of samples. The mineral is predominantly present as impregnations with sizes from 0.2 to 5 mm (in separate crystals, up to 2 cm). The cubic fluorite crystals often look like rounded grains due to flattened edges. The mineral color is light violet, violet, or sometimes spotty.

Table 4. Chemical compositions of Ba and Sr sulfates from the fluorite–barite–siderite carbonatites, wt %

Oxides	Barite	Sr-barite 4-7	Barytcelestine 4-1			4-3			Ba-celestine 4-2	4-4			4-8		Celestine
BaO	$\frac{62.4(6)}{60.2\text{–}65.0}$	45.8	24.7	26.0	28.0	28.3	$\frac{27.6(6)**}{22.4\text{–}34.3}$	$\frac{27.9(8)*}{23.4\text{–}31.5}$	4.8	6.2	6.3	8.2	12.1	12.3	$\frac{0.7(3)*}{0.34\text{–}1.3}$
SrO	$\frac{1.0(6)}{0.4\text{–}1.9}$	16.3	32.0	31.1	30.2	29.2	$\frac{31.1(6)}{27.0\text{–}37.2}$	$\frac{28.8(8)}{26.1\text{–}34.5}$	50.1	48.9	48.8	47.5	44.4	44.1	$\frac{54.2(3)}{52.6\text{–}56.0}$
CaO	$\frac{0.5(5)}{0.1\text{–}2.0}$	0.09	1.6	1.1	0.95	1.2		$\frac{2.5(8)}{1.3\text{–}3.4}$	0.14	0.21	0.15	0.44	0.10	0.10	$\frac{0.8(3)}{0.2\text{–}1.9}$
FeO	0,0n	0.10	–	0.06	0.15	0.14	1		0.15	0.14	0.04	0.68	0.30	1.06	0.02
MnO	0,0n–1	–	0.06	0.06	0.01	0.06	0.01		0.09	0.07	–	0.02	–	0.06	0.001
MgO	0,0n	–	–	0.01	0.03	–	0.01		0.10	0.12	0.12	0.03	0.06	0.09	<0.1
TiO$_2$	0,00n	0.37	0.08	0.44	0.30	0.32			–	0.14	0.09	0.10	0.14	0.20	
SiO$_2$	0.2–0.4	–	–	–	–	–	0.4		–	–	–	–	–	–	0.02
Al$_2$O$_3$	0,0n–1	0.09	0.14	0.11	0.02	–	0.08		–	0.02	0.02	–	–	0.04	0.02
TR$_2$O$_3$	0.05–0.12						0.2	0.14–0.36							0.02
SO$_3$		37.2	41.5	41.1	40.3	40.9		40.3	44.4	44.2	44.5	43.0	42.9	42.1	
Density, g/cm^3	4.35–4.23		4.19–4.14												4.03–3.97
a, Å	8.88–8.87		8.52–8.49												8.36–8.35
b, Å	5.48–5.45		5.41–5.40												5.37–5.34
c, Å	7.18–7.15		6.97–6.95												6.88–6.86
Ng	1.649–1.646		1.640–1.637												1.630–1.622
Np	1.637–1.635		1.631–1.627												1.622–1.620

* According to data of chemical analysis of mineral monofractions by A.S. Mitropolskii, D.O. Ontoev, A.P. Khomyakov, E.P. Nikolaeva, and A.V. Bolonin.

** Data of Nikolaeva *et al.* (1982).

Colorless and light green fluorite is observed in rare large impregnations. According to Khomyakov's data (1964), the density of violet fluorite is 3.12; that of green, 3.17; and that of colorless fluorite, 3.19 g/cm^3. In the matrix, fluorite forms small isometric and angular grains, disseminated in the siderite aggregate. According to scanning electron microscopy data, fluorites from impregnations (fluorite I) and from the matrix (fluorite II) differ only by FeO and SiO$_2$ content (Table 3). As a whole, fluorite from this deposit is characterized by a high contents (wt %) of TR$_2$O$_3$ (0.2–0.5), Y$_2$O$_3$ (0.1%), and SrO (0.1–0.5).

Barium and strontium sulfates have a widely varied chemical composition due to their cation isomorphism. Their composition and properties are presented in Table 4 and Fig. 3. In addition to the Karasug deposit data, the BaO–SrO–CaO chart (Fig. 3) includes data on chemical compositions of barium and strontium sulfates from the Late Mesozoic sulfates of the Western Transbaikal region (Nikiforov *et al.*, 2000; Ripp *et al.*, 2000) and the Mushugai deposit in Mongolia (Andreeva *et al.*, 1994), barite from hydrothermal deposits of Georgia (Uchameishvili *et al.*, 1980), and sulfates from an epigenetic celestine deposit in Turkey (Tekin *et al.*, 2002) (altogether 158 compositions). It follows from Fig. 3 that there are gaps in the chemical compositions in natural sulfates, and this fact forms a basis for the separation of intermediate varieties, for which the authors use the following names: barite–strontium barite (Sr-barite)–barytcelestine–barium celestine (Ba-celestine)–celestine. Note that, in most cases, in barytcelestine the celestine component predominates over the barite component and, therefore, the name "celestinbarite," sometimes used in the literature as a synonym for barytcelestine, should be recognized as less appropriate.

Barite content varies in ore-bearing carbonatites in the range 2–25%. It is mainly distributed in impregnations, its color is white, and its form is prismatic with size 0.5–5 mm (sometimes up to 3 cm). Lenticular barite crystal aggregates are occasional. Barite contains 1.0 wt % SrO and 0.5 wt % CaO. Porous and loose barite aggregates are occasional in the oxidation zone in limonitized ores. They are thought to be a product of strontium leaching in barytcelestine. There are two determinations of Ba and Sr sulfate compositions, which may be attributed to *Sr-barite* (Table 4; Fig. 3).

Barytcelestine is the main strontium mineral in ores. Barytcelestine forms pseudomorphs of light green color in white barite in many sectors of orebodies. Its fine-grained aggregates of light rose color substitute fluorite and siderite. The average strontium content in ores subjected to replacement by barytcelestine is 4–5 wt %, reaching 15 wt % in some places. The mineral has intermediate parameters of the unit cell, values of optical refraction, and density (Table 4). The sublinear dependence of parameters of unit cells of solid phases on their composition was calculated by Kotelnikov *et al.* (2000) on the basis of synthesized phases of BaSO$_4$–SrSO$_4$ solid solution taking into account data on natural sulfates, including those from the Karasug deposit.

Barium celestine is distinguished within the light rose aggregate of barytcelestine by results of electron microscope analysis. It forms aggregates of rich rose color. Figure 4 shows that barytcelestine fills central parts of mineral intergrowths and Ba-celestine is developed at their periphery.

Celestine of light blue color is observed as pseudomorphs in barite and as rare veinlets. It was determined that the veinlet celestine contains 0.8 wt % CaO and 0.7 wt % BaO.

On the basis of the morphology of aggregates, the Ba and Sr sulfates from the postmagmatic hydrothermal–metasomatic association are ranged in the following time series: barytcelestine–Ba celestine–celestine, reflecting the sequence of deeper replacement of the fluorite–barite–siderite carbonatites by strontium sulfate. All sulfates of the deposit, including the early barite, are characterized by a CaO content from 0.2 to 2.5 wt %.

Hematite forms dispersed impregnations of laminated metacrystals (specularite). Hematite bands are of black color; in some places, they are concentrated as pockets and veinlet segregations. Series of parallel veinlet hematite segregations result in ore banding. The size of hematite bands varies from $0.05 \times 0.2 \times 0.2$ to $1 \times 5 \times 5$ mm. Hematite is developed selectively in siderite. Its content in carbonatites subjected to hematitization (in ores of the fluorite–barite–hematite–siderite type) varies from 5 to 40 vol %, in local sectors being up to 65 vol %. The spectral analysis shows a gallium content in hematite reaching tens of grams per ton.

Bastnaesite in rocks is represented by two generations. The first generation of bastnaesite crystallized during the magmatic stage and forms single platy grains of yellow–brown color with sizes of from 0.04×0.1 to 1×5 mm. The mineral composition is presented in Table 5. The second generation of bastnaesite formed during the postmagmatic hydrothermal–metasomatic stage and is represented by platy metacrystals, by their sheaflike intergrowths, and by replacement fringes around fluorite impregnations. According to data of Khomyakov (1964), it contains (wt %) TR$_2$O$_3$, 75.8; CaO, 0.55; CO$_2$, 18.82; F, 8.90; and O=F$_2$, 3.74. The second generation of bastnaesite is associated with hematite and defines the enrichment of fluorite–barite–hematite–siderite ores by rare earth elements (TR$_2$O$_3$, 1.3–2.1 wt %) in comparison with fluorite–barite–siderite ores (0.7–1.2 wt %).

On the basis of radiographic analysis, thorium (0.3–0.6 wt % ThO$_2$) and uranium (0.07 wt % UO$_2$) are distributed uniformly, indicating an isomorphic character of their admixture (Bolonin, 1999). Bastnaesite is the main thorium concentrator in carbonatites; therefore, a direct correlation is statistically distinguished for contents of REE and thorium.
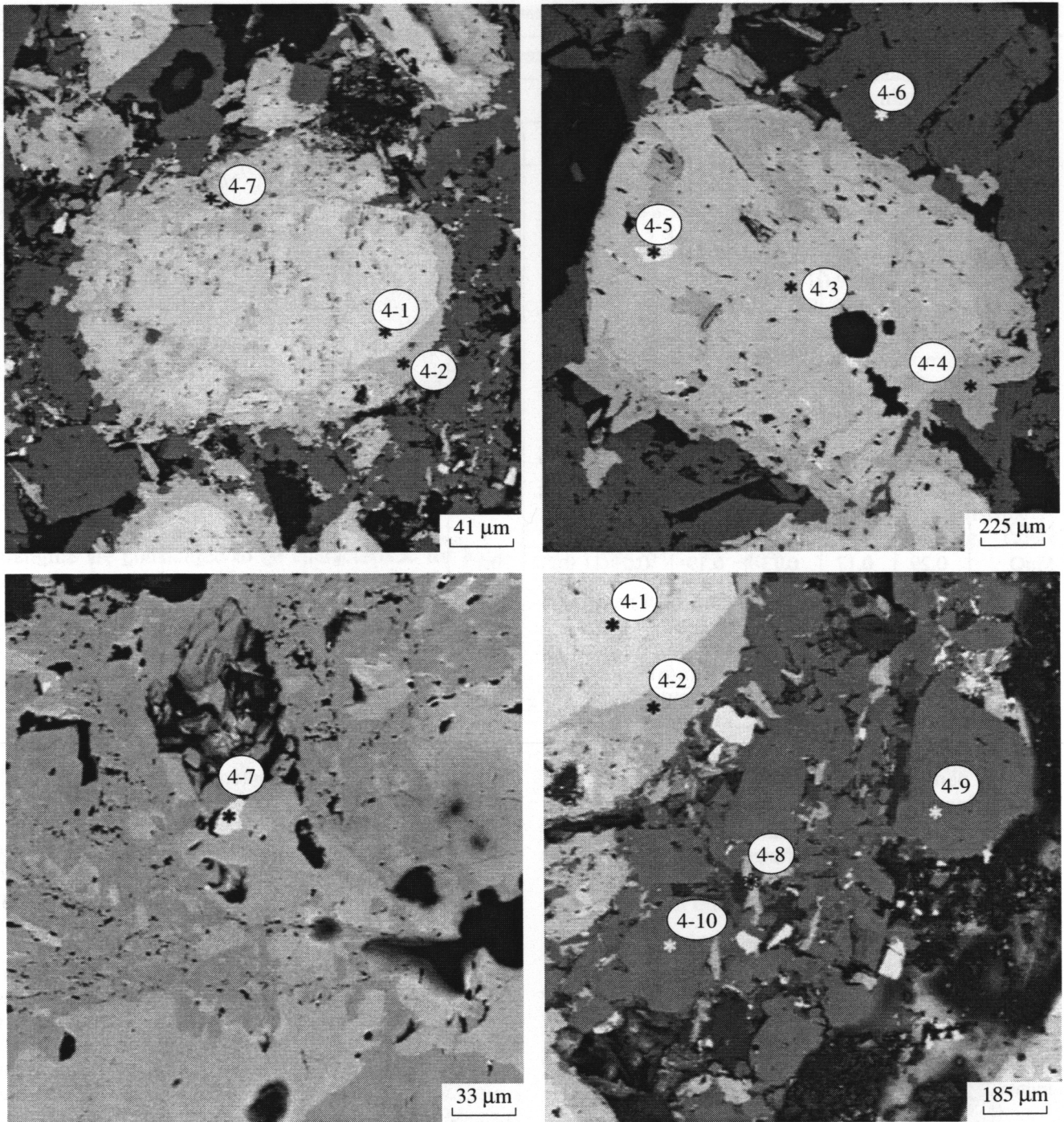
Fig. 4. Sections of fluorite–barite–siderite carbonatites scanned in reflected electrons. Here and further on, numbers of sampling points correspond to analysis numbers given in the tables. Minerals: siderite (4-6, 4-9, 4-10); barytcelestine (4-1, 4-3); Ba-celestine (4-2, 4-4, 4-8); Sr-barite (4-7); molybdenite (4-5).

The third generation of bastnaesite is observed in late hydrothermal quartz–siderite veinlets. According to data of A.S. Mitropolskii, S.V. Melgunov, and N.A. Kulik (1980), this bastnaesite contains (wt %) TR_2O_3, 73.81; CaO, 1.41; CO_2, 19.54; and F, 6.50.

Pyrite occurs in carbonatites in the amount of 0.2–4 vol % as impregnations 0.5–5 mm in size. The mineral has a complicated form with pentagonal dodecahedral planes. Pyrite contains 0.3–0.8 wt % Co with an insignificant content of Ni (<0.1 wt %) (Table 6). In

Table 5. Chemical compositions of fluorcarbonates of rare earths, wt %

Oxides	Fluorite–barite–siderite carbonatites								Ankerite–calcite carbonatites				
	bastnaesite I								parisite		roentgenite		synchisite
									9-4	9-1	9-5	9-2	9-3
La$_2$O$_3$	19.2	24.3	21.6	19.5	18.9	22.5	22.1		8.0	10.4	9.9	9.5	7.9
Ce$_2$O$_3$	36.8	36.3	35.5	36.6	35.9	35.1	31.4		20.9	25.2	24.1	24.1	18.0
Nd$_2$O$_3$	10.5	9.1	9.5	9.8	9.7	9.9	8.2		17.3	15.7	13.7	13.9	10.6
Y$_2$O$_3$	0.21	–	0.26	0.37	0.21	–	0.06		0.59	2.6	2.2	2.2	1.3
Al$_2$O$_3$	0.18	0.18	0.05	0.11	0.25	0.01	0.18	0.04*	0.20	0.17	0.30	0.16	0.26
ThO$_2$	–	1.6	0.54	0.41	–	0.41	0.87	0.16	0.65	0.80	2.0	2.6	3.4
UO$_2$	–	–	0.04	–	0.19	0.24	–	0.05					
TiO$_2$	–	0.10	0.20	0.14	0.03	–	–		0.07	0.03	0.15	0.11	0.00
SiO$_2$	0.20	0.07	0.23	0.25	0.29	0.19	0.19	0.2	–	0.25	–	0.22	0.04
CaO	0.25	0.32	0.89	0.08	0.10	0.15	0.16	0.6	11.1	12.2	12.8	13.8	22.8
MgO	–	0.06	–	0.02	–	–	–	0.2	0.03	0.10	0.10	0.15	0.08
MnO	0.29	0.17	0.13	0.19	0.21	0.21	0.15		–	–	–	–	–
FeO	–	0.38	0.01	–	–	0.06	0.10	0.7	–	–	0.10	0.94	3.1
SrO	0.35	0.41	0.08	0.21	0.22	0.27	0.24	0.16	–	0.24	–	0.17	0.43
BaO								0.04					

* According to data of two chemical analyses of monofractions by Khomyakov (1964) and Nikolaeva *et al.* (1982).

intensely hematitized carbonatites, the total amount of pyrite is increased to 5–7 vol % at the expense of its new generation, differing from the early pyrite by smaller size and by simpler form—cubic octahedral or cubic. Small grains of late pyrite are distinguished in

Table 6. Chemical compositions of pyrite and molybdenite, wt %

Elements	Ankerite–calcite carbonatites	Fluorite–barite–siderite carbonatites		
	impregnated pyrite	impregnated pyrite	late pyrite	molybdenite
				4-5
S	52.9	52.9	53.2	40.1
Fe	46.7	46.3	46.5	0.15
Co	0.18	0.78	0.01	–
Ni	0.07	0.03	0.11	–
Cu	0.07	–	0.07	–
Zn	0.08	0.01	0.09	0.05
Mo				59.7

celestinized ores. Low contents of nickel and cobalt were determined in its composition, with Ni > Co (Table 6). A high cobalt concentration (Co ≫ Ni) in early magmatic pyrite at the deposit is reflected in the bulk ore composition, containing 0.012 wt % Co and only 0.001 wt % Ni. In the oxidation zone, pyrite is replaced by a compact aggregate of goethite and hydro-goethite.

Magnetite is occasionally observed in primary carbonatites in the form of octahedral impregnations. The spectral analyses reveal a low content of admixtures in magnetite, including Al < 0.05 and Ti < 0.1 wt %, which explains the absence of exsolution textures in the mineral. The other form of magnetite is platelike pseudomorphs in hematite (muschketowite). Only rare hematite plates are replaced by magnetite.

Uraninite forms disseminated impregnations of the finest (<0.1 mm) grains, confined to the fine-grained carbonatites and distinguished in f-gamma ray images (Fig. 5). Only large uraninite crystals of cubic form are observed under a microscope, in a brown radiation aureole in siderite and a dark violet aureole in fluorite. Microprobe analyses revealed the following uraninite composition (wt %): UO$_2$, 93.8; ThO$_2$, 2.0; Y$_2$O$_3$, 1.0; Ce$_2$O$_3$, 0.4; La$_2$O$_3$, 0.3; Al$_2$O$_3$, 0.3; Cr$_2$O$_3$, 0.2; SiO$_2$, 0.3; TiO$_2$, 0.1; FeO, 0.8; CaO, 0.4; and SrO, 0.1. High contents of yttrium, REE, and thorium distinguished in
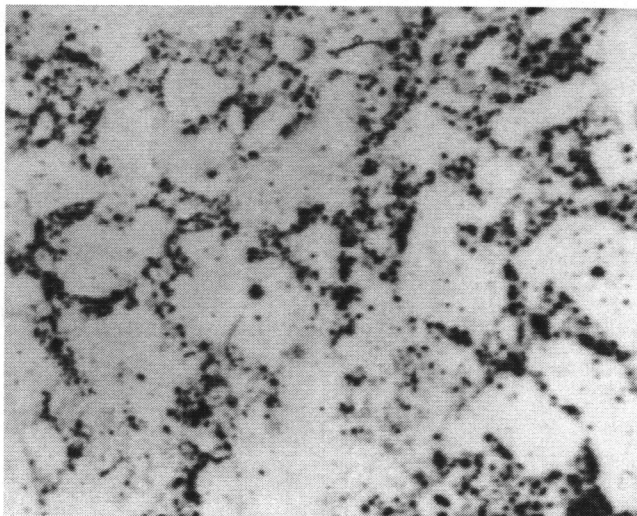
Fig. 5. F-radiography of porphyraceous fluorite–barite–siderite carbonatites. Magnification 2. Black, tracks from uraninite in the ground mass.

uraninite are considered to be characteristic for high-temperature uraninites (from granites, pegmatites, and greisens) in contrast to hydrothermal uranium oxides (Mineev, 1974). Uraninite is dissolved in the oxidation zone and the uranium is sorbed by Fe hydroxides, from which it is easily leached.

Molybdenite forms a constant admixture of fine hexagonal flakes, confined to the carbonatite matrix. An insignificant admixture of Fe (0.15 wt %) and Zn (0.05 wt %) is distinguished in it (Table 6).

Chalcopyrite, sphalerite, galenite, and marcasite are occasional in hydrothermally altered carbonatites, being associated with barytcelestine, quartz, and quartz–siderite veinlets. Primary contents of elements of the latter sulfides are insignificant (wt %): Cu and Zn, 0.004, and Pb, 0.001.

Apatite is represented by fine (0.1–1 mm in length) hexagonal columnar crystals disseminated in carbonatites. Its content in carbonatites is from several fractions to 4 vol %.

Muscovite is observed in the form of colorless and light green hexagonal–platy impregnations with a size of up to 1–3 mm. The chemical composition of muscovite is the following according to the microprobe analysis data (wt %): K_2O, 10.9; Na_2O, 0.1; Al_2O_3, 28.8; SiO_2, 47.5; TiO_2, 0.8; FeO, 6.3; MnO, <0.1; CaO, 0.3; and MgO, 0.8. The crystallochemical formula of muscovite is the following: $(K_{0.94}Na_{0.01}Ca_{0.02})_{0.97}(Al_{1.47}Fe'''_{0.35}Ti_{0.04}Mg_{0.08})_{1.94}(Si_{3.19}Al_{0.81})_4$ $O_{10}(OH)_2$. A high content of iron and a low content of magnesium in muscovite is explained by the paragenesis of this mica with siderite. In optical parameters (Ng, 1.607; Nm, 1.604; $2V = 15°–20°$), the ferrous muscovite differs from the common muscovite, distributed in fragments of greisenized granites (Ng, 1.606; Np, 1.566; $2V = 39°–40°$).

Quartz in an amount up to 5 vol % is common in carbonatites in the form of dipyramidal hexagonal–prismatic light gray crystals with sizes up to 10 mm and elongation from 1 : 2 to 1 : 4. It is represented by the low-temperature modification (β-quartz, <573°C), confirmed by x-ray data. Note that the well-shaped crystals with two tops, regularly dispersed in the fluorite–barite–siderite carbonatites, were formed at the stage of magmatic crystallization.

The late hydrothermal silicification was manifested locally in near-contact parts of some carbonatite bodies in siderite carbonatites, shown by replacement of rocks by fine-grained quartz aggregates.
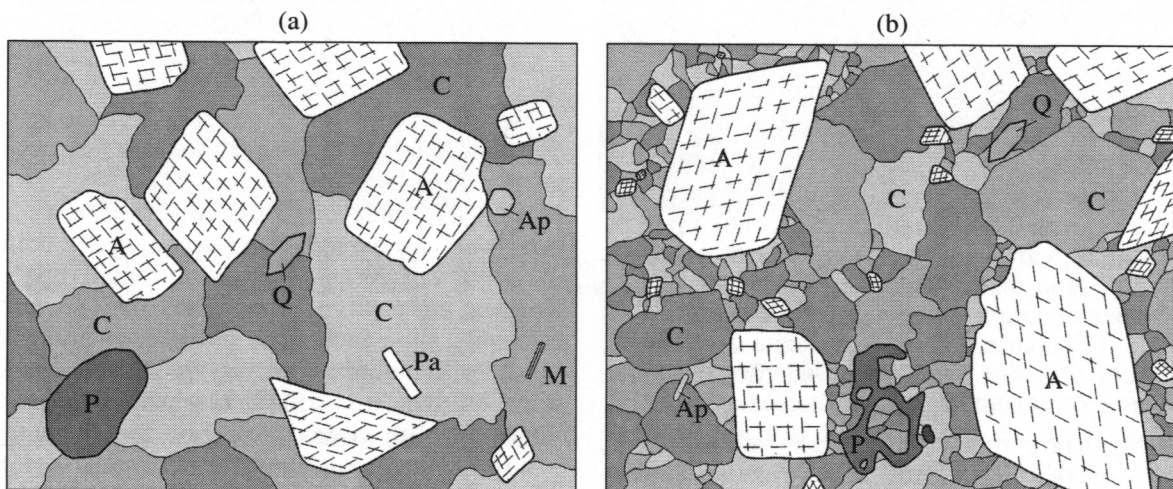
(a)   (b)

Fig. 6. Primary subhedral (a) and porphyraceous (b) structure of the ankerite–calcite carbonatites. Magnification 10. Minerals: A, ankerite; C, calcite; P, pyrite; Pa, parisite; Ap, apatite; Q, quartz; M, muscovite.
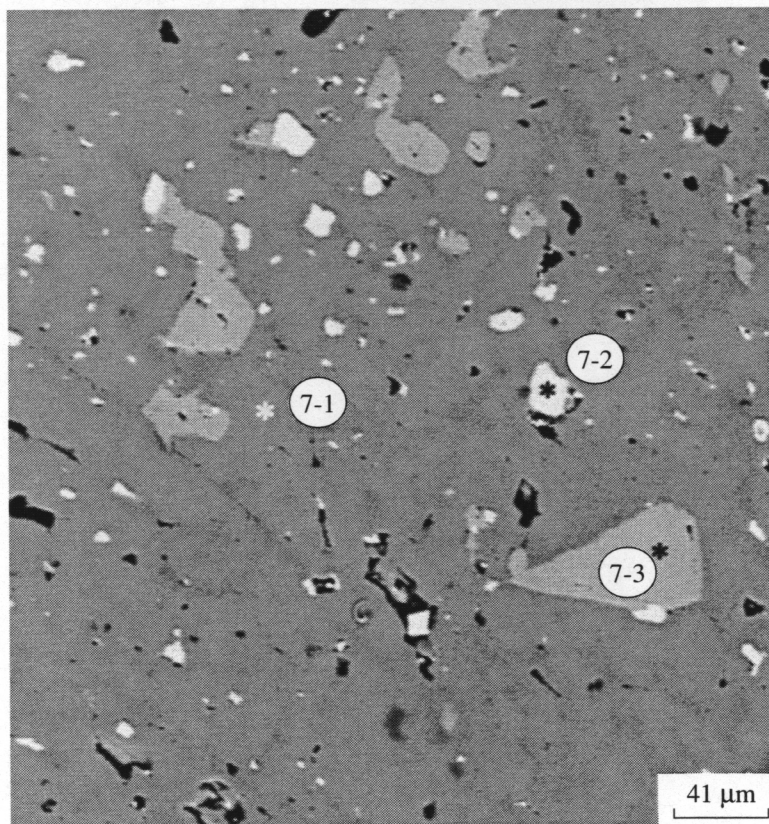
Fig. 7. Image in reflected electrons of a calcite crystal (dark, 7-1) with inclusions of Mg-siderite (white, 7-2), and ankerite (gray, 7-3) from ankerite–calcite carbonatites.

Note that the greater part of SiO_2 and Al_2O_3, fixed in large-volume ore samples (8–15 wt % SiO_2 and 2.3–6 wt % Al_2O_3), is associated with fragments of granitoids, sandstones, and siltstones in the ore mass.

Rutile in the form of fine inclusions is observed sometimes in quartz and muscovite impregnations. Its presence in the carbonatites is most probably associated with reworking of host rock fragments.

Ankerite–Calcite Carbonatites

The ankerite–calcite carbonatites are rocks of white color with equigranular, subhedral, and locally porphyraceous textures (Fig. 6). The size of carbonate grains varies from 0.5 to 2 mm, being locally up to 5–7 mm. In these carbonatites, the content of calcite is 60–45 vol % and that of ankerite, 50–35 vol %. The sum of other minerals is about 5 vol %: apatite, 1–2; pyrite, 0.5–1.5; quartz, 1–2; and monazite and parisite, 0.5. Muscovite, rutile, magnetite, siderite, dolomite, chalcopyrite, molybdenite, and thorite are sporadic.

Postmagmatic hydrothermal–metasomatic processes, widely developed in fluorite–barite–siderite carbonatites, practically did not occur in ankerite–calcite carbonatites. Along with this, strontianite is common among their oxidized varieties, and celestine and cal-

cite are distributed as veinlets. The content of strontianite replacing the ground mass is locally up to 30 vol %.

Calcite is represented by an aggregate of grains with irregular isometric form and polysynthetic twinning. The mineral is of white color, and its refraction parameters are as follows: Ng, 1.66; Np, 1.49. According to data of Khomyakov (1964) the parameters of the unit cell are as follows: $a = 4.99$ Å, $c = 17.06$ Å, and density 2.73 g/cm^3; chemical analysis of the monofraction revealed a high content of FeO, MnO, and MgO (3.88, 0.23, and 1.79 wt %, respectively). The authors obtained considerably lower content in calcite from the analyzed sample (wt %): FeO, 0.83; MnO, 0.17; and MgO, 0.07 (Table 2). At the same time, unusual structures were discovered during scanning of calcite grains in reflected electrons. They contain small (up to 10 μm) irregular ingrowths of magnesian siderite in addition to relatively large inclusions of ankerite grains (Fig. 7; Table 2). Such ingrowths may be interpreted as syngenetic, but then it is still unclear why siderite is absent outside calcite grains. Probably, the exsolution of a solid carbonate solution of complicated composition takes place, similar to that described in rocks of the Murun massif (Konev *et al.*, 1996). In any case, these inclusions may partially absorb iron and magnesium, a
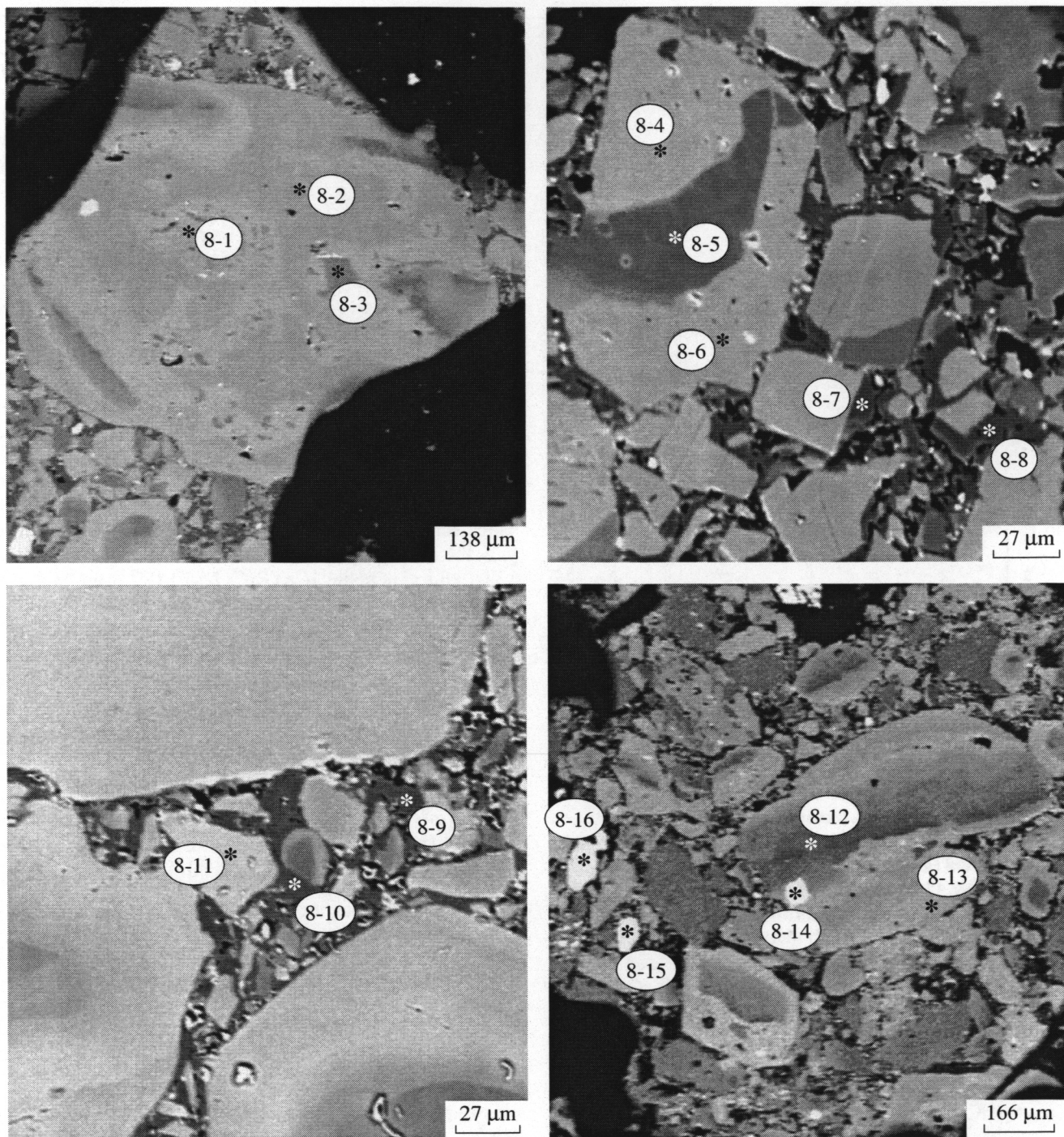
Fig. 8. Ankerite–calcite carbonatites scanned in reflected electrons. Ankerite I (8-3, 8-5, 8-12), ankerite II (8-1, 8-2, 8-4, 8-6, 8-11, 8-13), dolomite (8-7, 8-8, 8-9, 8-10), apatite (8-15, 8-16), monazite (8-14).

high content of which is characteristic for high-temperature calcite (Talantsev, 1981).

In the oxidation zone, calcite often includes microinclusions of hydrogoethite, providing the mineral with a light brown color.

Ankerite forms regularly distributed rhombohedral crystals and smaller grains and their aggregates in calcite aggregates. The refraction value of the mineral is $Ng = 1.71$–1.73. A sharp inhomogeneity of chemical composition was distinguished during ankerite scanning with the electron microscope (Fig. 8): dark zones in the crystal nucleus correspond to ankerite I, in which Fe and Mg contents are consistent (average 15.1 wt % FeO and 10.7 wt % MgO), and light zones (ankerite II)

Table 7. Chemical composition of monazite and apatite from ankerite–calcite carbonatites, wt %

Oxides	Monazite			Apatite			
			8-14	8-16	8-15		
SO_3	0.65	0.65	0.45	–	1.3	–	–
P_2O_5	29.7	31.2	29.8	36.4	35.8	37.3	36.0
ThO_2	6.9	3.0	7.7	0.01	–	0.07	0.05
UO_2	0.03	0.49	0.29				
SiO_2	0.72	0.10	0.89	–	0.07	0.05	–
TiO_2				0.04	–	0.08	–
Al_2O_3	0.21	0.15	0.10	–	0.04	0.13	0.09
La_2O_3	10.7	10.9	9.4	0.10	0.08	0.39	0.24
Ce_2O_3	30.5	31.8	30.2	0.39	0.49	0.65	0.56
Nd_2O_3	19.1	20.7	19.7	0.52	0.27	0.27	0.27
Y_2O_3	–	–	–	–	–	–	–
SrO	0.67	0.45	0.54	0.77	0.48	0.65	0.57
FeO	–	–	–	0.41	0.27	0.31	0.23
MnO				–	–	–	0.02
CaO	0.77	0.54	0.81	56.2	55.6	56.2	56.1
MgO				0.02	–	–	

in the outer rim fix a sharp predomination of Fe over Mg (28.6 wt % FeO and 2.1 wt % MgO) (Table 2). Khomyakov (1964) gave the following characteristics for ankerite from the monofraction: CaO, 33.96; FeO, 11.52; MgO, 10.37; MnO, 0.34; and TR_2O_3, 0.05 wt %; density, 3.01 g/cm^3. These data are the closest to ankerite I.

In the oxidation zone, hydrogoethite is developed after ankerite, first along the contour of grains and cleavage cracks of ankerite; ankerite then disappears completely with the formation of pseudomorphs composed of hydrogoethite and secondary calcite.

Dolomite was distinguished in ankerite–calcite carbonatites for the first time by electron scanning. This mineral forms small (<0.02 mm) irregular aggregates between ankerite and calcite grains (Fig. 8). The following contents were determined in dolomite (wt %): MgO, 17.5; FeO, 2.1; MnO, 0.1; and SrO, 0.47 (Table 2).

Apatite is represented by colorless hexagonal–columnar crystals 0.1–1 mm long, regularly dispersed in the ground rock mass. It is fluoroapatite ($Ng = 1.633$, $Np = 1.629$, density 4.8 g/cm^3), containing 0.9–1.3 wt % $(La + Ce + Nd)_2O_3$ and 0.5–0.8 wt % SrO (Table 7).

Monazite is a common accessory mineral of ankerite–calcite carbonatites. It is represented by fine platy grains 0.02–0.5 mm in size of yellow or rose color. Monazite is the main concentrator of thorium in ankerite–calcite carbonatites; it contains 3–7.7 wt % ThO_2 and up to 0.5 wt % UO_2 (Table 7). According to data of Nikolaeva *et al.* (1982), 1 wt % ThO_2 and 0.07 wt % UO_2 were determined in monazite.

Parisite is represented by fine platy crystals of yellow color ($No = 1.677$). The microprobe analysis revealed a high content of CaO—11.1–12.2 wt %—as compared with the theoretical content of 10.4 wt % according to its chemical formula $[CaTR_2(CO_3)_3F_2]$. Notable is a content of yttrium in parisite at a level of 0.6–2.6 wt % Y_2O_3, which corresponds to a high concentration of heavy lanthanides in it in comparison with bastnaesite and monazite (Khomyakov, 1964). In one case, the electron scanning (Fig. 9a) revealed the replacement of parisite at the crystal periphery and in cleavage cracks by secondary fluorcarbonates of REE. The replacing mineral is close to roentgenite $[Ca_2TR_3(CO_3)_5F]$ (12.8–13.8 wt % CaO; theoretically, 13.6) and synchisite $[CaTR(CO_3)_2F]$ (22.8 wt % CaO; theoretically, 17.5) in calcium content (Table 5). In the other case (Fig. 9b), such replacement was not observed for the crystal edges and the roentgenite formed the internal zone. All fluorcarbonates have a close correlation for La, Ce, and Nd.

Thorite is sporadic. According to data of Nikolaeva *et al.* (1982), it is represented by prismatic crystals up to 0.5 mm long, of green and blue color, and its density is 6.4 g/cm^3. The following were determined in its composition (wt %): U, 3.1; Fe, 4; Ca, 1.5; P, 1; Sr, 1; Ba, 0.2; Ce, 0.7; La, 0.1; Y, 0.7; and Al, 0.7.

Pyrite has a complicated form with pentagonal faces as in siderite carbonatites, and it is often intensely corroded by calcite. The Co content is also higher than that for nickel: 0.18 wt % Co and 0.07 wt % Ni (Table 6).

Muscovite is observed in the form of hexagonal plates of light color with the optical parameters $Ng = 1.609$ and $2V = 40°–50°$.

Quartz, as in fluorite–barite–siderite carbonatites, is represented by well-formed dipyramidal hexagonal–prismatic crystals up to 10 mm in size, uniformly dispersed throughout the entire rock mass.

Rutile is found in insignificant inclusions in calcite. The following were determined by microprobe analysis (wt %): TiO_2, 97.01; CaO, 1.5; Cr_2O_3, 1.1; and FeO, MgO, and SiO_2, about 0.1.

Chalcopyrite and molybdenite are sporadic, and the content of chalcophile elements in carbonatites is insignificant: Cu, 0.002; Zn and Co, 0.0015; and Mo and Pb, 0.000*n* wt %.
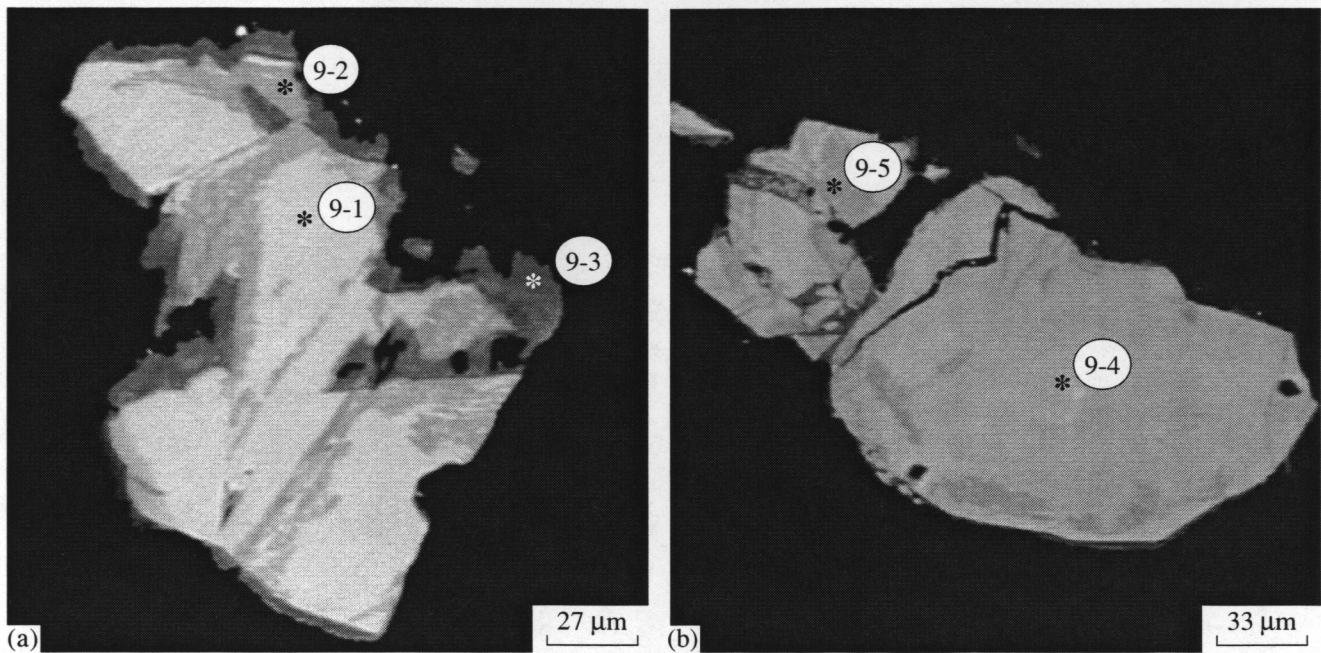
Fig. 9. Images in reflected electrons of parisite crystals (a, b). Parisite (9-1, 9-4), roentgenite (9-2, 9-5), and synchisite (9-3).

DISCUSSION

Typomorphic minerals of ankerite–calcite carbonatites of the Karasug deposit are calcite, ankerite, apatite, muscovite, quartz, parisite, monazite, and pyrite, and those for fluorite–barite–siderite carbonatites are siderite, fluorite, Ba and Sr sulfates, bastnaesite, apatite, quartz, ferrous muscovite, pyrite, molybdenite, and uraninite. Carbonatites of both varieties with different composition of the rock-forming minerals have the same set of subordinate minerals and are characterized by a high content of iron, REE, and radioactive elements. They have a high content of strontium (0.1–0.6 wt % SrO) in calcium-bearing and rare earth minerals (carbonates, fluorocarbonates, fluorite, monazite, and apatite).

A specific feature of carbonatites in the Karasug deposit is the relation of quartz to typomorphic minerals. Quartz is represented by dipyramidal hexagonal–prismatic crystal impregnations, formed during the magmatic stage. The muscovite type of mica is also unusual because phlogopites and rarer biotite are distributed in carbonatites of the world among micas. The high content of molybdenum in fluorite–barite–siderite carbonatites of the deposit in the form of molybdenite and cobalt in pyrite may be accepted as a feature characteristic for ferrous carbonatites, as was shown by Frolov *et al.* (2003). The presence of uraninite in fluorite–barite–siderite carbonatites as the main uranium-bearing mineral phase is unusual. Thorium minerals (thorite, thorianite, and uranothorianite) are usually mentioned in carbonatites of other massifs of the world among minerals containing uranium as an isomorphic admixture. In the Karasug deposit, uranium formed its own mineral phase, first, because of the high primary uranium content and low thorium–uranium ratio (0.15–0.7), and, second, due to the deposition of radioactive elements during different stages (thorium in the bastnaesite impregnations, and uranium during crystallization of porphyraceous fluorite–barite–siderite carbonatites).

The absence of such minerals as chlorite, sericite, and rhodochrosite in the composition of carbonatites is characteristic for the Karasug deposit. These minerals were considered in other carbonatite massifs as exclusively hydrothermal minerals (Samoilov, 1984; Frolov *et al.*, 2003). Barite cannot be related to them. Evidence for the possibility of magmatic genesis of sulfates, except the Karasug deposit (Bolonin, 1983), has been found by a number of researchers: Andreeva *et al.* (1994) discovered celestine and anhydrite in South Mongolia in the carbonatite-bearing massif Mushugai–Khuduk in apatite in molten inclusions together with silicates and calcite; Konev *et al.* (1996) found prismatic crystals of barytcelestine in leucitic lamproites of the Murun alkaline massif, which crystallized directly from a melt; and Nikiforov *et al.* (2000) considered prismatic crystals of barytcelestine as phenocrysts in eruptive calcite carbonatites of the Khalyutin complex in the Western Transbaikal region. Magmatic anhydrite was described by Andrew *et al.* (2000) in granites and by Luhr and Logan (2002) in trachyandesites.

According to the mineral composition, the Karasug deposit is in a series of such carbonatite complexes of the world as Mushugai in Mongolia, Khalyutin and Arshan in the Western Transbaikal region, Malomurun in the Aldan Shield, and the Mountain Pass deposit in

North America. Each of these objects is peculiar, but all of them are characterized by a high level of concentration of barium, strontium, LREE, fluorine, and sulfur in rocks. At the mineral level, this is expressed in the saturation of many minerals by the elements mentioned, which in most cases form their own mineral phases (sulfates or carbonates of Ba and Sr, monazite, TR fluorcarbonates, and fluorite). Thus, the mineral composition of rocks and chemical compositions of minerals in the Karasug deposit are typical for REE carbonatites.

The analyses performed enabled us to characterize the chemical compositions of main rock-forming minerals of carbonatites of the Karasug deposit. It was established that minerals of variable compositions were widely developed in addition to rock-forming minerals of constant compositions. The minerals of variable compositions are carbonates of the ankerite–dolomite series, REE fluorcarbonates of the parisite–roentgenite–synchisite series from the ankerite–calcite carbonatites, and barium and strontium sulfates from the fluorite–barite–siderite carbonatites.

ACKNOWLEDGMENTS

REFERENCES

1. I. A. Andreeva, V. B. Naumov, V. I. Kovalenko, et al., "Magmatic Celestine in Molten Inclusions in Apatites of the Alkaline Volcano-Plutonic Mushugai–Khuduk Complex (Southern Mongolia)," Dokl. Ross. Akad. Nauk **337** (4), 499–502 (1994).

2. P. Andrew, Barth, and M. J. Dorais, "Magmatic Anhydrite in Granitic Rocks: First Occurrence and Potential Petrologic Consequences," Am. Mineral. **85** (3–4), 430–435 (2000).

3. A. V. Bolonin, "Geochemical Features of Carbonatites of the Complex Iron–Fluorite–Barite–Rare Earths Deposit," Izv. Vyssh. Uchebn. Zaved. Razved., No. 1, 19–24 (1987).

4. A. V. Bolonin, "Rare Earths, Yttrium, Uranium, Thorium, and Strontium in Ores of the Karasug Carbonatite Deposit in Tuva," Rudy Met., No. 6, 31–43 (1999).

5. A. A. Frolov, A. V. Tolstov, and S. V. Belov, *Carbonatite Deposits of Russia* (NIA-Priroda, Moscow, 2003) [in Russian].

6. A. P. Khomyakov, "Mineralogy and Distribution of Rare Elements in One of Rare Earth Fluorocarbonate Deposits," in *Mineralogy and Genetic Features of Alkaline Massifs* (Nauka, Moscow, 1964) [in Russian].

7. A. A. Konev, E. I. Vorob'ev, and K. A. Lazebnik, *Mineralogy of the Murun Alkaline Massif* (Novosibirsk, Izd. SO RAN, NITs OIGGM, 1996) [in Russian].

8. A. R. Kotelnikov, Yu. K. Kabalov, T. N. Zezyulya, et al., "Experimental Study of the Solid Celestine–Barite Solution," Geokhimiya, No. 12, 1286–1293 (2000).

9. J. F. Luhr and M. A. V. Logan, "Sulfur Isotope Systematics of the 1982 El Chichon Trachyandesite: An Ion Microprobe Study," Geochim. Cosmochim. Acta **66** (8), 3303–3316 (2002).

10. D. A. Mineev, *Lanthanides in Ores of Rare Earths and Complex Ore Deposits* (Nauka, Moscow, 1974) [in Russian].

11. A. S. Mitropolskii, "Hydrothermal Complex Iron Ore Deposits," in *Iron Ore Deposits of the Altai–Sayany Mountain Region* (Akad. Nauk SSSR, Moscow, 1959), Vol. 1, book 2 [in Russian].

12. A. S. Mitropolskii, "About Ancient Oxidation Zones in Deposits of Carbonatite Ores of Western Tuva," Geol. Geofiz., No. 1, 19–23 (1962).

13. A. V. Nikiforov, V. V. Yarmolyuk, B. G. Pokrovskii, et al., "Late Mesozoic Carbonatites of Western Transbaikal Region: Mineral, Chemical, and Isotopic (O, C, S, Sr) Compositions and Relation with Alkaline Magmatism," Petrologiya **8** (3), 309–336 (2000).

14. E. P. Nikolaeva, A. A. Brovkin, N. G. Barsuk, et al., "Study of Minerals of the Barite–Celestine Series from Oxidized Complex Ores," in *Radiography Analysis of Mineral Resources* (VIMS, Moscow, 1982), pp. 93–104.

15. D. O. Ontoev, *Geology of Complex Rare Earths Deposits* (Nedra, Moscow, 1984) [in Russian].

16. G. S. Ripp, O. V. Kobylkina, A. G. Doroshkevich, and A. O. Sharakshinov, *Late Mesozoic Carbonatites of the Western Transbaikal Region* (Ulan-Ude Izd-vo BNTs SO RAN, 2000) [in Russian].

17. V. S. Samoilov, *Geochemistry of Carbonatites* (Nedra, Moscow, 1984) [in Russian].

18. A. S. Talantsev, *Geothermobarometry by Dolomite–Calcite Parageneses* (Nauka, Moscow, 1981) [in Russian].

19. E. Tekin, B. Varol, I. S. Sayili, and Y. Elerman, "Indications of Intermediate Compositions in the $BaSO_4$–$SrSO_4$ Solid-Solution Series from the Bahceciktepe Celestine Deposit, Sivas, East-Central Anatolia, Turkey," Can. Mineral. **40**, 895–908 (2002).

20. N. E. Uchameishvili, S. D. Malinin, and N. I. Khitarov, *Geochemical Data on Processes of the Barite Deposit Formation* (Nauka, Moscow, 1980) [in Russian].